Advances in Machinery, Materials Science and Engineering Application
M. Chen et al. (Eds.)

doi:10.3233/ATDE220477

Vibration Transfer Analysis of a Passive Hybrid Vibration Isolation System Based on Impedance Synthesis Method

Junde MA [a,1], Haiwei WANG [b] and Yafeng REN [c]
[a] *Xi'an Aerospace Propulsion Test Technology Institute, Xi'an 710100, China*
[b] *Northwestern Polytechnical University, Xi'an 710072, China*
[c] *Taiyuan University of Science and Technology, Taiyuan, 030024, China*

Abstract. Precision instrument will be disturbed by the vibration of mechanical equipment in the working process, which will deteriorate its normal operation and delay the test progress. So, it needs to be protected by vibration isolation device. In this paper, a hybrid vibration isolation platform is proposed which contains a high static low dynamic quasi-zero stiffness isolation system and a passive bilayer isolation system. And a fully flexible impedance dynamic model is established for this system based on the impedance synthesis method. The vibration transfer characteristics of the hybrid platform under the real excitation of the engine testbed are analyzed and verified by relevant tests. Results show that the designed vibration isolation device has fine broadband vibration isolation effect and can meet the usage requirements.

Keywords. Precision instrument, vibration isolation device, impedance synthesis approach, vibration transmission, quasi-zero stiffness vibration isolator

1. Introduction

The health monitoring of mechanical equipment and the effective collection of test data are inseparable from precision measuring instruments. Precision instruments such as data collectors, charge amplifiers, high-speed cameras and UPS power supplies are often vulnerable. Severe vibration generated by mechanical equipment in the process of operation will be transmitted to the precision instrument through the foundation platform, too high vibration will not only damage the instrument itself, but also deteriorate the test data and even delay the overall test progress. Using vibration isolation measures to cut back the impact of environmental vibration on preciseness instruments is an efficient methodology, especially for the already designed or even built test bench, this is almost the only way.

Conventional passive vibration isolation system can be classified into single-layer isolation system and double-layer isolation system according to the different number of isolator layers. Double-layer isolation system has higher vibration isolation ability than single-layer isolation system at high frequency, which has been wide employed in automobile, ship and other fields. Wang [1] and Zhang [2] et al discussed in detail the

[1] Junde Ma, Corresponding author, Xi'an Aerospace Propulsion Test Technology Institute, Xi'an 710100, China; E-mail: 263359070@qq.com

influence of equipment parameters, vibration isolator parameters, raft parameters and foundation parameters on vibration isolation performance. For the rigid body vibration isolation model, decrease the stiffness of the upper and lower isolators will increase the vibration isolation effect, but too small isolators' stiffness will induce poor stability of the equipment. With the emergency of large-scale isolation system, the influence of flexibility of equipment, raft and foundation is increasingly prominent. Sciulli and Inman [3] believed that the elasticity of the machine will significantly influence the natural properties of the system. Niu and Song [4] established a flexible dynamic model for general isolation systems, and discussed the influence rules of machine flexibility and foundation flexibility on the force transmissibility. Results show that both machine and foundation flexibility make the transmissibility curve larger and produce new peaks. Li [5] et al analyzed the influence rules of foundation stiffness and excitation frequency changes on different isolation evaluation indexes.

Conventional vibration isolation systems are linear, which will face a hard nut to crack at low-frequency. Zhao [6] et al developed a quasi-zero stiffness (QZS) isolation system with small space occupation and convenient installation by paralleling the vertical spring with two symmetrical negative stiffness structures, which has fine stability and low-frequency isolation performance. Li [7] combined a double-layer isolation system with a high static and low dynamic stiffness isolation system, proposed a double-layer high static and low dynamic stiffness isolation system, and compared its vibration isolation performance with the ordinary bilayer linear isolation system. Results show that the isolation performance is the best when the upper stiffness is completely linear, and the lower stiffness is quasi zero.

In order to realize smart broadband vibration isolation results, a passive hybrid vibration isolation platform is projected in this paper which contains a QZS isolator and a bilayer isolation platform. Then the impedance synthesis approach is adopted to build the full flexible impedance dynamic model of the hybrid vibration isolation platform. Finally, the vibration transmission characteristics of the system are analyzed, and the analytical results are verified by experiments.

2. Model Description

The hybrid vibration isolation platform shown in figure 1 is adopted, including a bilayer isolation platform and a QZS isolation platform. The double-layer isolation platform is used to isolate wide-frequency and large amplitude vibration, and the QZS vibration isolation platform is used to further isolate low-frequency vibration. The bilayer isolation platform mainly includes an upper table, four upper vibration isolators, a lower table, four lower vibration isolators and an outrigger. The dimensions of upper and lower worktops are both 0.4 m × 0.6 m. The thickness of the upper table is 10 mm and the thickness of the lower table is 8 mm. The quasi zero vibration isolation platform mainly consists of four horizontal springs and a vertical spring.

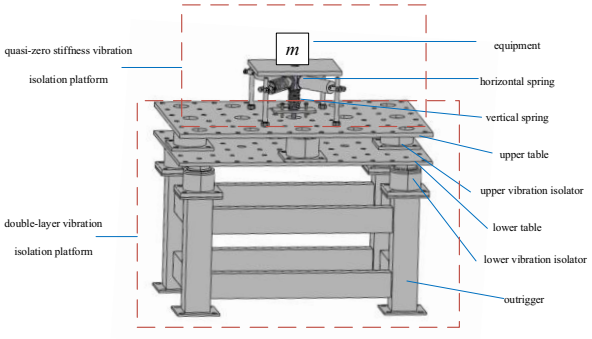

Figure 1. Model of vibration isolation device.

3. Dynamic Modeling of Hybrid Vibration Isolation Device

3.1. Impedance Modeling of Subsystems

3.1.1. Instruments and Equipment

The size of the instrument is small and its own stiffness is large, so it is simplified as a lumped mass block, and the equation of motion is:

$$\boldsymbol{M}^{\mathrm{yq}}\ddot{\boldsymbol{x}}^{\mathrm{yq}}(\mathrm{t}) = \boldsymbol{f}^{\mathrm{yq}}(\mathrm{t}) \tag{1}$$

where, $\boldsymbol{M}^{\mathrm{yq}}$ is the mass matrix of the instrument, $\boldsymbol{x}^{\mathrm{yq}}$ is the node displacement vector of the instrument, $\boldsymbol{f}^{\mathrm{yq}}(t)$ is the exciting force vector of the instrument, and here is the reaction force from the upper table to the instrument and equipment.

The impedance equation of the instrument system yields:

$$\boldsymbol{Z}^{\mathrm{yq}}(\omega)\boldsymbol{V}^{\mathrm{yq}}(\omega) = \boldsymbol{F}^{\mathrm{yq}}(\omega) \tag{2}$$

where, $\boldsymbol{Z}^{\mathrm{yq}}$ is the impedance matrix, $\boldsymbol{Z}^{\mathrm{yq}}(\omega) = \mathrm{j}\omega\boldsymbol{M}^{\mathrm{yq}}$. $\boldsymbol{V}^{\mathrm{yq}}$ is the velocity vector of the instrument system in the frequency domain, $\boldsymbol{V}^{\mathrm{yq}}(\omega) = \mathrm{j}\omega\boldsymbol{X}^{\mathrm{yq}}(\omega)$. $\boldsymbol{X}^{\mathrm{yq}}(\omega)$ is the frequency domain form of $\boldsymbol{x}^{\mathrm{yq}}(\mathrm{t})$. $\boldsymbol{F}^{\mathrm{yq}}$ is the excitation force vector of the instrument system in the frequency domain.

3.1.2. QZS Vibration Isolator

The dynamic model of QZS vibration isolator is shown in figure 2. The horizontal springs are used as the negative stiffness regulating mechanism, and the vertical spring is employed as the positive stiffness regulating mechanism. The solid line represents the free state of the system before loading, and the dotted line represents the static equilibrium state of the system after loading. m is the bearing mass; k_v and k_h are the stiffness of vertical and horizontal spring respectively; L is the initial length of the

horizontal spring, and l is its condensed length at the horizontal position; c_v is the vertical damping coefficient.

The equivalent dimensionless stiffness of the QZS vibration isolator can be yielded as [6]:

$$\hat{K} = \frac{\mathrm{d}\hat{F}}{\mathrm{d}\hat{x}} = (1+\beta) - \frac{\beta\alpha^2}{\left(\hat{x}^2 + \alpha^2\right)^{\frac{3}{2}}} \tag{3}$$

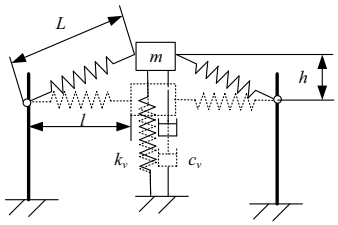

Figure 2. Dynamic model of QZS isolator.

In our model, the stiffness of the vertical spring is 0.7×10^3 N/m, the stiffness of the four horizontal springs is 1.06×10^3 N/m. The dimensionless stiffness - displacement curve is shown in figure 3.

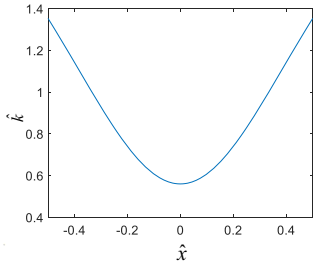

Figure 3. Dimensionless stiffness - displacement curve.

The dynamic behavior of QZS vibration isolator shows certain nonlinear characteristics when the vibration is large [6]. In this paper, due to the vibration isolation effect of the bilayer isolation table, the vibration transmitted to the QZS isolator is very small, that is, the dimensionless displacement is between -0.01 ~0.01, so it is assumed that the stiffness of the QZS isolator is a constant value, and the system is linear.

The dynamic model of the QZS isolator can be simplified into two parts, one is a lumped mass block composed of a small platform and a connecting structure, and the other is an equivalent spring composed of a horizontal spring and a vertical spring. Its impedance equation can be described as follows:

$$\boldsymbol{Z}^{\mathrm{qzs}}(\omega)\boldsymbol{V}^{\mathrm{qzs}}(\omega) = \boldsymbol{F}^{\mathrm{qzs}}(\omega) \tag{4}$$

where, $\boldsymbol{Z}^{\mathrm{qzs}}$ is the impedance matrix of the quasi-zero stiffness isolator, $\boldsymbol{Z}^{\mathrm{qzs}}(\omega)=\mathrm{C}^{\mathrm{qzs}}+\mathrm{j}\omega\mathrm{M}^{\mathrm{qzs}}+\mathrm{K}^{\mathrm{qzs}}/(\mathrm{j}\omega)$. $\boldsymbol{V}^{\mathrm{qzs}}$ is the vibration velocity. $\boldsymbol{F}^{\mathrm{qzs}}$ is the applied force.

3.1.3. Upper Table

The upper table is a continuum and is modeled by finite element (FE) method, as shown in figure 4. The middle surface of the upper table is extracted and meshed by the quadrilateral shell element. The element size is 5mm. The material density is 7850 kg/m^3, the modulus of elasticity is 2.1×10^{11} Pa and the Poisson's ratio is 0.3. Washers are established at the installation holes of the instrument and vibration isolator to improve the quality of local grid, center nodes are created in the center of the hole and MPC constraints are used to couple the center nodes with the nodes on the hole. The installation points of the instrument and vibration isolators are defined as the external nodes of the upper table. Modal analysis is performed and modal parameters within 10000Hz are extracted.

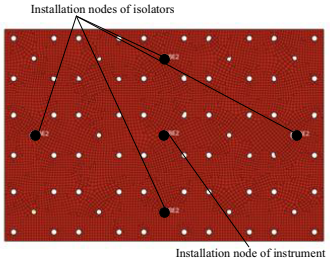

Figure 4. FE model of the upper table.

The upper table contains five external nodes, and each node considers three translational degrees of freedom. Therefore, the mobility matrix of the upper table can be expressed as a 15×15 matrix.

$$[Y]=\begin{bmatrix} Y_{11} & Y_{12} & \cdots & Y_{1n} \\ & Y_{22} & \cdots & Y_{2n} \\ & & \ddots & \vdots \\ \mathrm{Sym.} & & & Y_{nn} \end{bmatrix} \tag{5}$$

Each mobility element Y_{lp} represents the velocity response at point l caused by applying unit force at point p, which can be calculated by Eq.(6).

$$Y_{lp}(\omega)=\mathrm{j}\omega\sum_{r=1}^{n}\frac{u_l^r u_p^r}{K_r-\omega^2 M_r+\mathrm{j}\omega C_r} \tag{6}$$

where, K_r is the modal stiffness of the upper table, M_r is the modal mass of the upper table, C_r is the modal damping of the upper table, u is the vibration mode shape, r is the modal order, l is the external node number, p is the freedom p=x, y, z.

The impedance matrix of the upper table can be obtained by inverse the mobility matrix:

$$\boldsymbol{Z}^{\mathrm{stm}}(\omega)=\boldsymbol{Y}^{\mathrm{stm}}(\omega)^{-1} \tag{7}$$

Then, the impedance equation of the upper table can be obtained:

$$\boldsymbol{Z}^{\mathrm{stm}}(\omega)\boldsymbol{V}^{\mathrm{stm}}(\omega)=\boldsymbol{F}^{\mathrm{stm}}(\omega) \tag{8}$$

where, $\boldsymbol{Z}^{\mathrm{stm}}$ is the impedance matrix of external nodes of the upper table, $\boldsymbol{V}^{\mathrm{stm}}$ is the velocity vector of external nodes of the upper table, and $\boldsymbol{F}^{\mathrm{stm}}$ is the reaction force of instruments and vibration isolators on external nodes of the upper table.

3.1.4. Vibration Isolators

Vibration isolators are selected according to the bearing capacity, as is shown in figure 5. Four air spring vibration isolators HF-1-5525 are used for the upper vibration isolators. And four air spring vibration isolators ALJ-51001 are used for the lower vibration isolators.

(a) Upper vibration isolator (b) Lower vibration isolator

Figure 5. Photograph of the isolators.

The masses of the isolators are small, so they can be considered as the spring damping elements. Take the vibration isolator of the upper layer as an example, and its movement equation is:

$$\boldsymbol{C}^{\mathrm{sgzq}}\dot{\boldsymbol{x}}^{\mathrm{sgzq}}(\mathrm{t})+\boldsymbol{K}^{\mathrm{sgzq}}\boldsymbol{x}^{\mathrm{sgzq}}(\mathrm{t})=\boldsymbol{f}^{\mathrm{sgzq}}(\mathrm{t}) \tag{9}$$

where, $\boldsymbol{C}^{\mathrm{sgzq}}$ is the damping matrix of the upper vibration isolator, $\boldsymbol{K}^{\mathrm{sgzq}}$ is the stiffness matrix of the upper vibration isolator, $\boldsymbol{x}^{\mathrm{sgzq}}$ is the node displacement vector of the upper vibration isolator, $\boldsymbol{f}^{\mathrm{sgzq}}(t)$ is the exciting force vector of the upper vibration isolator system, and here is the reaction force of the upper and lower table on the upper vibration isolator.

In the frequency domain, the impedance equation of the upper vibration isolators can be yielded:

$$\boldsymbol{Z}^{\mathrm{sgzq}}(\omega)\boldsymbol{V}^{\mathrm{sgzq}}(\omega)=\boldsymbol{F}^{\mathrm{sgzq}}(\omega) \tag{10}$$

where, $\boldsymbol{Z}^{\mathrm{sgzq}}$ is the impedance matrix, $\boldsymbol{Z}^{\mathrm{sgzq}}(\omega)=\boldsymbol{C}^{\mathrm{sgzq}}+\boldsymbol{K}^{\mathrm{sgzq}}/(\mathrm{j}\omega)$. $\boldsymbol{V}^{\mathrm{sgzq}}$ is the velocity vector of the upper vibration isolator system, $\boldsymbol{V}^{\mathrm{sgzq}}(\omega)=\mathrm{j}\omega\boldsymbol{X}^{\mathrm{sgzq}}(\omega)$. $\boldsymbol{X}^{\mathrm{sgzq}}(t)$ is the frequency domain form of $\boldsymbol{x}^{\mathrm{sgzq}}(t)$. $\boldsymbol{F}^{sgzq}$ is the excitation force vector in the frequency domain of the upper vibration isolator.

Similarly, the impedance equation of the lower isolator can be obtained:

$$\boldsymbol{Z}^{\mathrm{xgzq}}(\omega)\boldsymbol{V}^{\mathrm{xgzq}}(\omega)=\boldsymbol{F}^{\mathrm{xgzq}}(\omega) \tag{11}$$

3.1.5. Lower Table

The FE model of the lower table is shown in figure 6. Quadrilateral shell element is used for mesh generation, with mesh size of 5mm, material density of 7850 kg/m^3, and modulus of elasticity of 2.1×10^{11} Pa, Poisson's ratio 0.3. The upper and lower isolator mounting points are defined as the external nodes of the lower table surface by establishing a washer at the mounting holes of isolators to improve the local mesh quality, creating a node at the center of the hole and coupling it with the nodes on the hole through the rbe2 element.

Modal analysis is carried out on the lower table and modal information below 10000Hz is extracted. The mobility elements of the external nodes of the lower table are calculated by modal parameters, and the impedance parameters are obtained by matrix inversion, and then the impedance equation of the lower table can be obtained:

$$\boldsymbol{Z}^{\mathrm{xtm}}(\omega)\boldsymbol{V}^{\mathrm{xtm}}(\omega)=\boldsymbol{F}^{\mathrm{xtm}}(\omega) \tag{12}$$

where, $\boldsymbol{Z}^{\mathrm{xtm}}$ is the impedance matrix of the external nodes of the lower table, $\boldsymbol{V}^{\mathrm{xtm}}$ is the velocity vector of the external nodes of the lower table, and $\boldsymbol{F}^{\mathrm{xtm}}$ is the reaction force of isolators on the external nodes of the lower table.

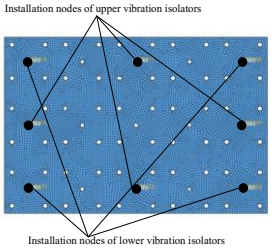

Figure 6. FE model of the lower table.

3.1.6. Outrigger

The mid plane of the outrigger is extracted, and the quadrilateral shell element is used for mesh generation. The FE model is shown in figure 7. The mesh size is 5 mm. The material density is7850 kg/m^3. The modulus of elasticity is 2.1×10^{11} Pa. The Poisson's ratio is 0.3. The lower isolator mounting point is defined as the external nodes of the lower table surface by establishing a washer at the mounting hole of the lower isolator to improve the local grid quality, creating a node at the center of the hole and coupling it with the node on the hole through the rbe2 element. At the same time, the contact

surface between the outrigger and the ground is coupled to the corresponding central nodes, which are also defined as external nodes.

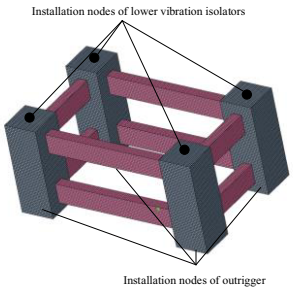

Figure 7. FE model of the outrigger.

Modal analysis is performed on the outrigger and modal parameters within 10000Hz are extracted. The mobility element of the external nodes of the outrigger can be calculated by modal parameters, and the impedance parameters can be obtained by matrix inverse, and then the impedance equation of the outrigger could be obtained:

$$\boldsymbol{Z}^{\mathrm{zt}}(\omega)\boldsymbol{V}^{\mathrm{zt}}(\omega) = \boldsymbol{F}^{\mathrm{zt}}(\omega) \tag{13}$$

where, $\boldsymbol{Z}^{\mathrm{zt}}$ is the impedance matrix of the external nodes of the outrigger, $\boldsymbol{V}^{\mathrm{zt}}$ is the velocity vector of the external nodes of the outrigger, and $\boldsymbol{F}^{\mathrm{zt}}$is the reaction force of the lower vibration isolator and the steel plate foundation on the external nodes of the outrigger.

3.1.7. Vibration Transferring Analysis of the Coupled System

Impedance synthesis is carried out by the method of reference [8]. Through the impedance equation, force balance equation and motion coordination equation of the subsystems, the impedance equation of the coupled system yields:

$$\boldsymbol{ZV} = \boldsymbol{F} \tag{14}$$

The foundation vibration acceleration is the excitation source of the whole system, and its magnitude can be measured by test. In Eq.(14), the foundation vibration velocity can be obtained by vibration acceleration conversion:

$$\tilde{\boldsymbol{V}}^{\mathrm{gb}}(\boldsymbol{\omega}) = \tilde{\boldsymbol{A}}^{\mathrm{gb}}(\boldsymbol{\omega}) / (\mathrm{j}\boldsymbol{\omega}) \tag{15}$$

In Eq.(14), the impedance matrix is a known quantity, and the vibration velocity of the steel plate foundation in the velocity vector is also a known quantity. Therefore, the vibration velocity could be obtained.

The vibration isolation efficiency can be described by the acceleration transmissibility:

$$\begin{cases} T_{A,x} = A_x^{yq} / A_{b,x}^{zt} \\ T_{A,y} = A_y^{yq} / A_{b,y}^{zt} \\ T_{A,z} = A_z^{yq} / A_{b,z}^{zt} \end{cases} \tag{16}$$

where, T_A is the acceleration transmissibility, A^{yq} is the vibration acceleration of the instrument or equipment, and A_b^{zt} is the vibration acceleration of the mounting points of the outrigger.

3.2. Validation

To calculate the vibration isolation efficiency of the proposed platform under the real excitation of the engine test bench, the characteristic data of the foundation vibration acceleration measured in the test is brought into the model, and the vibration of the instrument can be obtained, as shown in figure 8. The rms of the foundation vibration acceleration is 42.60g, the rms of the instrument vibration acceleration is 1.26g, so the comprehensive vibration isolation efficiency is 97.03%, that is, the comprehensive vibration isolation amount is 30.5dB, meeting the vibration isolation demand.

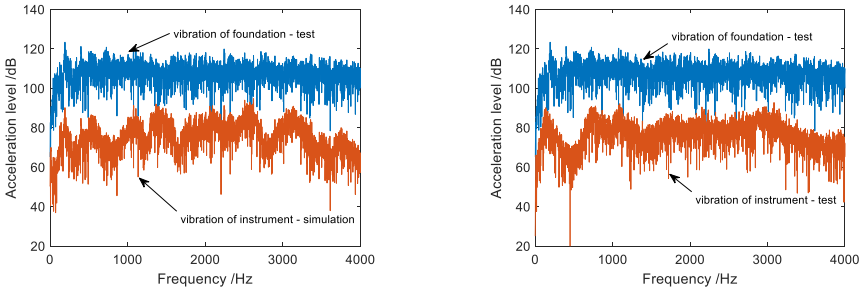

(a) Analytical results (b) Experimental results

Figure 8. Comparison of vibration acceleration between simulation and experiment.

4. Conclusion

A combined platform with a quasi-zero stiffness isolator and bilayer isolation system is designed, and the full flexible dynamic model of the platform is built by using the impedance synthesis approach. By analyzing the vibration transmission properties of the whole isolation system, the results show that the designed vibration isolation platform can meet the vibration isolation requirements, and the comprehensive acceleration transmissibility under the real excitation of the engine test-bed can reach 30.5dB.

Acknowledgments

This study is supported by the Natural Science Foundation of Shanxi Province (20210302124445) and the Excellent Doctoral Scientific Research Starting Foundation of Shanxi Province (20202061).

References

[1] Wang GZ and Li LB. Research on influences on dynamical characteristics of ship floating raft. Shipbuilding of China. 2002; 01:45-53.
[2] Zhang HL, Fu ZF and Qu ZQ. The effects of parameters of floating raft isolation system on its isolation characteristics. Journal of Vibration and Shock. 2000; 19(2):5-8, 4.
[3] Sciulli D, Inman DJ. Isolation design for full flexible systems. J. Intel. Mater. Syst. Struct. 1999; 10: 813-824.
[4] Niu JC and Song KJ. Transmission characteristics of fully flexible isolation systems subjected to multi-excitations and supported by multi-mounts. Journal of Mechanical Engineering. 2011; 47(7): 59-64.
[5] Li YC, Weng ZY, Tang J, You HW. Evaluation of vibration isolation effect of double-layer isolation systems with flexible foundations. Noise and Vibration Control. 2018; 38(06): 172-177.
[6] Zhao Q, Li SH, Feng GZ. Design and test of a quasi-zero-stiffness vehicle vibration isolation system. Journal of Vibration and Shock; 2021; 40(06): 55-63+183.
[7] Li YY, Zhou XB, Chen WD, Liu XT. Dynamic characteristics and application restrictions of a two-stage vibration isolation system with high-static-low-dynamic Stiffness. Journal of Vibration Engineering. 2021; 34(02): 364-371.
[8] Ren YF, Chang S, Liu G, and Wu LY. Impedance Synthesis Based Vibration Analysis of Geared Transmission System. Shock and Vibration. 2017; 3:1-14.